

Electronic Supporting Information

Solution-processed OLEDs Based on Phosphorescent PtAu₂ Complexes with Phenothiazine-functionalized Acetylides

Xian-Chong Zeng,^{a,b} Jin-Yun Wang,^a Liang-Jin Xu,^a Hui-Min Wen^{*,a} and
Zhong-Ning Chen^{*a,b}

^a *State Key Laboratory of Structural Chemistry, Fujian Institute of Research on the Structure of Matter, Chinese Academy of Sciences, Fuzhou, Fujian 350002, China. E-mail: czn@fjirsm.ac.cn.*

^b *College of Chemistry, Fuzhou University, Fuzhou, Fujian 350002, China.*

Table S1. Crystallographic data for 2·3CH₂Cl₂.

empirical formula	C ₁₀₇ H ₈₈ Au ₂ Cl ₈ N ₂ O ₈ P ₆ PtS ₂
formula weight	2652.36
crystal system	triclinic
space group	$P \bar{1}$
a , Å	12.7978(1)
b , Å	14.9854(3)
c , Å	16.8833(3)
α , deg	84.385(8)
β , deg	74.318(8)
γ , deg	70.229(7)
V , Å ³	2933.52(8)
Z	1
ρ_{calcd} g/cm ⁻³	1.501
μ , mm ⁻¹	4.034
radiation (λ , Å)	0.71073
temp,(K)	293(2)
R1 (F_o) ^a	0.0489
wR2 (F_o^2) ^b	0.1440
GOF	0.995

^a $R1 = \Sigma|F_o - F_c|/\Sigma F_o$

^b $wR2 = \Sigma[w(F_o^2 - F_c^2)^2]/\Sigma[w(F_o^2)]^{1/2}$

Table S2. The partial molecular orbital compositions (%) and the absorption transitions for complex **1** in CH₂Cl₂ media calculated by TD-DFT method at the PBE1PBE level.

orbital	energy (eV)	MO contribution (%)			
		Pt (s/p/d)	Au (s/p/d)	dpmp	C≡C-PTZ-Et
LUMO+7	-1.37	13.58 (0/100/0)	9.41 (34/51/15)	63.07	13.94
LUMO+4	-1.49	3.48 (0/100/0)	3.31 (29/37/34)	89.96	3.25
LUMO+2	-1.64	2.17 (0/100/0)	10.70 (21/64/15)	83.69	3.44
LUMO	-2.50	14.16 (0/100/0)	22.87 (61/30/9)	53.93	9.04
HOMO	-5.47	5.29 (5/0/95)	0.59 (55/20/25)	1.27	92.85
HOMO-2	-6.53	13.70 (3/0/97)	2.41 (58/7/35)	3.27	80.61
HOMO-3	-6.65	34.22 (22/0/78)	38.58 (36/10/54)	25.58	1.63

states	<i>E</i> , nm (eV)	O.S.	transition (Contrib.)	assignment	exp. (nm)
S ₁	509 (2.44)	0.5101	HOMO→LUMO (97%)	¹ LLCT/ ¹ LMCT	479
S ₄	374 (3.32)	0.2143	HOMO→LUMO+2 (57%) HOMO-3→LUMO (16%)	¹ LLCT/ ¹ LMCT ¹ MC/ ¹ MLCT/ ¹ IL	
S ₅	370 (3.35)	0.4991	HOMO-3→LUMO (71%) HOMO→LUMO+2 (15%)	¹ MC/ ¹ MLCT/ ¹ IL ¹ LLCT/ ¹ LMCT	382
S ₇	365 (3.40)	0.313	HOMO-2→LUMO (74%) HOMO-3→LUMO (11%)	¹ LLCT/ ¹ LMCT/ ¹ MC ¹ MC/ ¹ MLCT/ ¹ IL	

Table S3. The partial molecular orbital compositions (%) and the emission transition for complex **1** in CH₂Cl₂ media calculated by TD-DFT method at the PBE1PBE level.

orbital	energy (eV)	MO contribution (%)			
		Pt (s/p/d)	Au (s/p/d)	dpmp	C≡C-PTZ-Et
LUMO	-2.72	16.07 (0/100/0)	25.51 (68/22/10)	49.85	8.57
HOMO	-5.31	4.57 (2/0/98)	0.57 (54/24/23)	1.18	93.69

states	<i>E</i> , nm (eV)	O.S.	transition (contrib.)	assignment	exp. (nm)
T ₁	672 (1.84)	0.0000	HOMO→LUMO (83%)	³ LLCT/ ³ LMCT	683

Table S4. The partial molecular orbital compositions (%) and the absorption transitions for complex **2** in CH₂Cl₂ media calculated by TD-DFT method at the PBE1PBE level.

orbital	energy (eV)	MO contribution (%)			
		Pt (s/p/d)	Au (s/p/d)	dpmp	C≡CC ₆ H ₄ -PTZ
LUMO+7	-1.45	10.84 (0/97/3)	8.81 (42/42/16)	63.30	17.05
LUMO+4	-1.55	4.61 (6/55/39)	5.17 (34/44/22)	85.17	5.05
LUMO	-2.61	14.96 (0/99/0)	24.06 (62/30/9)	50.25	10.73
HOMO	-5.71	0.20 (30/7/63)	0.13 (73/15/12)	0.09	99.58
HOMO-2	-6.52	25.77 (10/0/90)	2.40 (57/17/26)	3.17	68.66
HOMO-3	-6.72	34.02 (22/0/78)	38.97 (37/10/53)	25.92	1.09

states	<i>E</i> , nm (eV)	O.S.	transition (Contrib.)	assignment	exp. (nm)
S ₁	460 (2.70)	0.0392	HOMO→LUMO (97%)	¹ LLCT/ ¹ LMCT/ ¹ IL	448
S ₃	393 (3.15)	0.4982	HOMO-2→LUMO (96%)	¹ LLCT/ ¹ MC/ ¹ LMCT	382
S ₄	374 (3.32)	0.6567	HOMO-3→LUMO (98%)	¹ MC/ ¹ MLCT/ ¹ IL	

Table S5. The partial molecular orbital compositions (%) and the emission transition for complex **2** in CH₂Cl₂ media calculated by TD-DFT method at the PBE1PBE level.

orbital	energy (eV)	MO contribution (%)			
		Pt (s/p/d)	Au (s/p/d)	dpmp	C≡CC ₆ H ₄ -PTZ
LUMO	-2.88	16.50 (0/100/0)	25.87 (67/22/10)	48.12	9.51
HOMO	-5.52	0.10 (83/2/15)	0.07 (90/9/1)	0.06	99.76

state	<i>E</i> , nm (eV)	O.S.	transition (contrib.)	assignment	exp. (nm)
T ₁	610 (2.03)	0.0000	HOMO→LUMO (95%)	³ LLCT/ ³ LMCT	572

Table S6. Optimization of electroluminescent performance of OLEDs based on complex **1**.

dopant	host	doping (%)	λ_{EL} (nm)	V_{on} (V)	L_{max} (cd m ⁻²)	CE_{max} (cd A ⁻¹)	PE_{max} (lm W ⁻¹)	EQE^a (%)	EQE^b (%)
1	TAPC	8	595	5.60	1402	14.4	5.3	6.7	2.1
1	TAPC : OXD-7 (48% : 47%)	5	605	5.05	6263	16.4	5.8	7.6	7.2
1	TAPC : OXD-7 (46% : 46%)	8	605	4.50	10446	35.4	16.8	18.7	16.9
1	TCTA : OXD-7 (46% : 46%)	8	606	4.85	8594	25.8	12.0	13.1	11.8
1	mCP : OXD-7 (46% : 46%)	8	605	5.65	3112	3.7	1.4	2.0	1.7
2	TCTA : OXD-7 (46% : 46%)	8	568	4.95	8975	21.7	9.7	8.0	6.9
2	TAPC : OXD-7 (46% : 46%)	8	568	4.60	3940	20.0	10.2	7.1	5.6

^a The highest external quantum efficiency. ^b External quantum efficiency at brightness of 1000 cd m⁻².

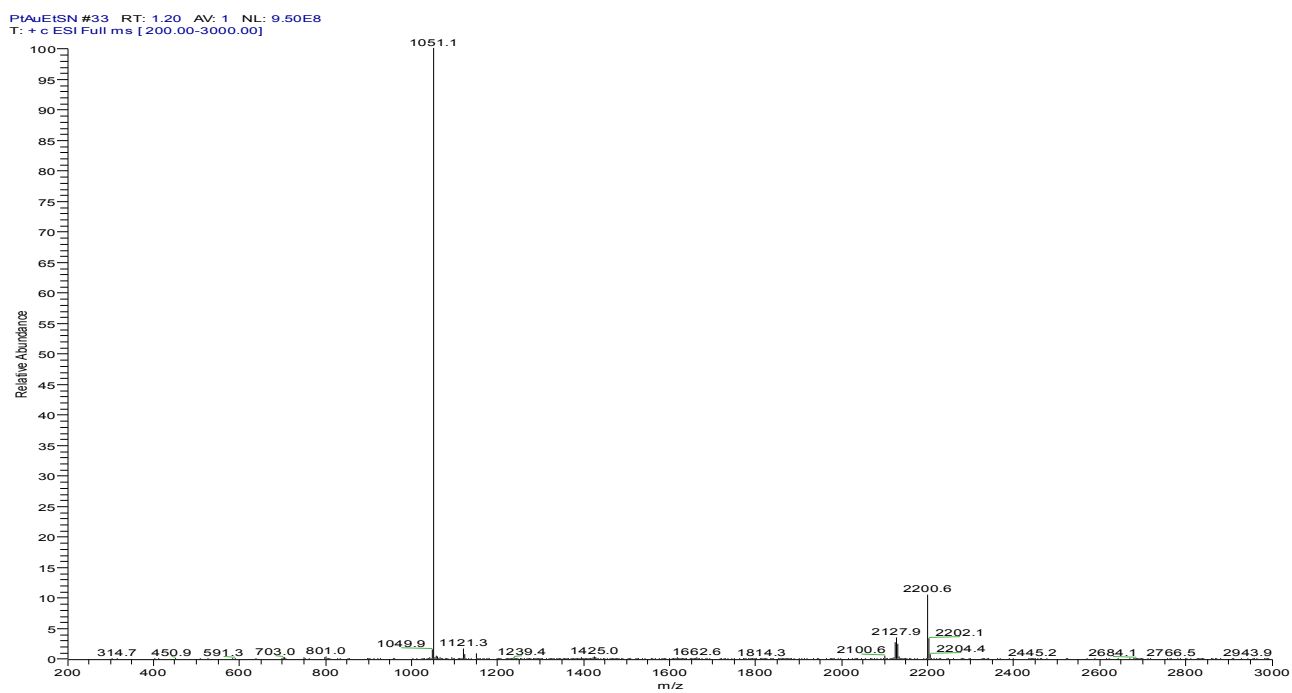


Figure S1. The ESI-MS of complex 1.



Figure S2. The ESI-MS of complex 2.

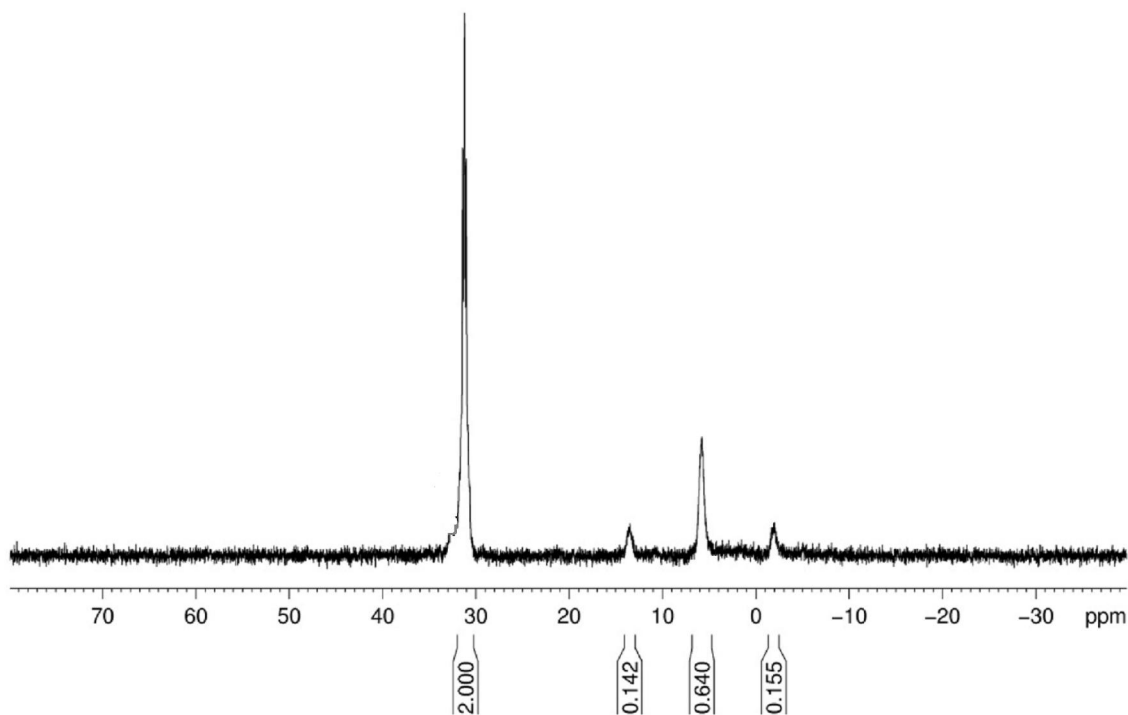


Figure S3. The ^{31}P NMR spectrum of complex 1.

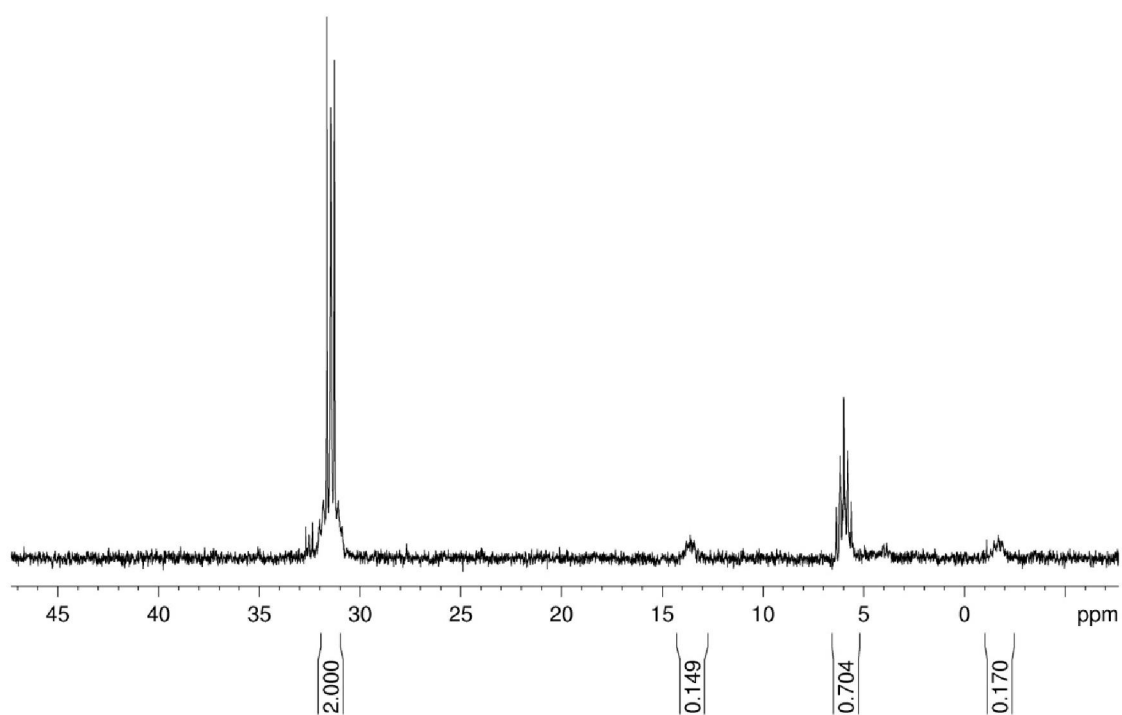


Figure S4. The ^{31}P NMR spectrum of complex 2.

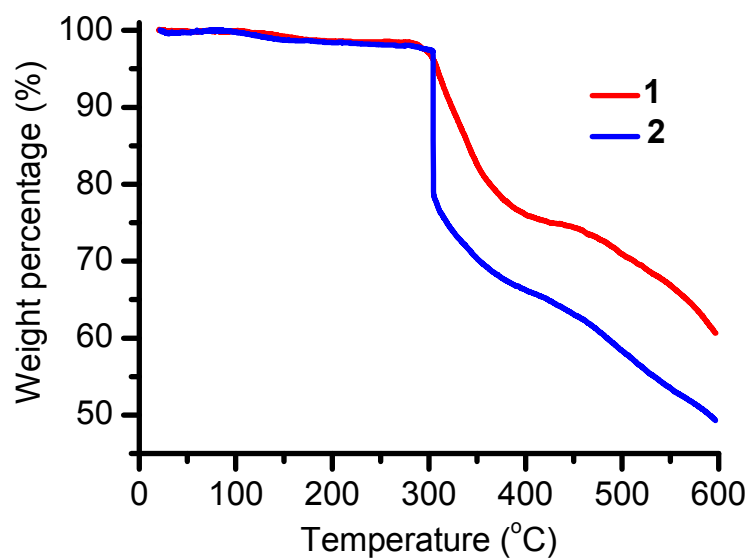


Figure S5. Plots of thermogravimetric analysis for complexes **1** and **2** in temperature range 25-600 °C.

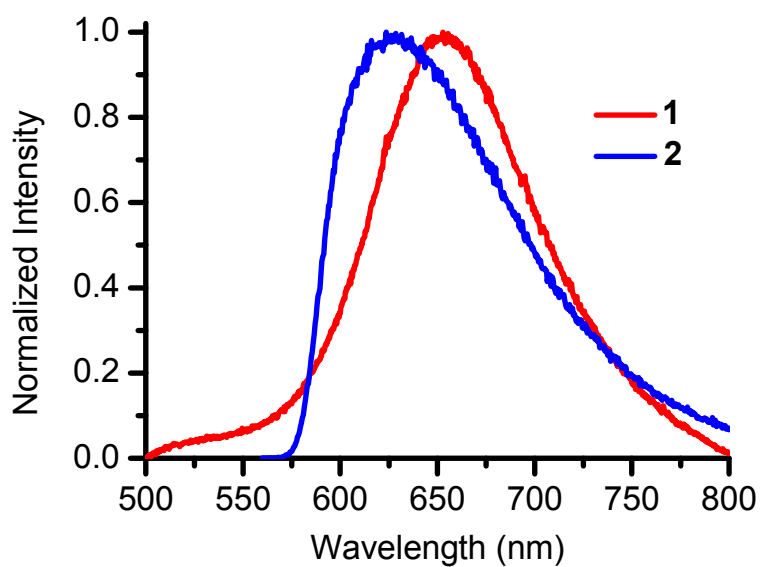


Figure S6. The emission spectra of complexes **1** and **2** in powder state.

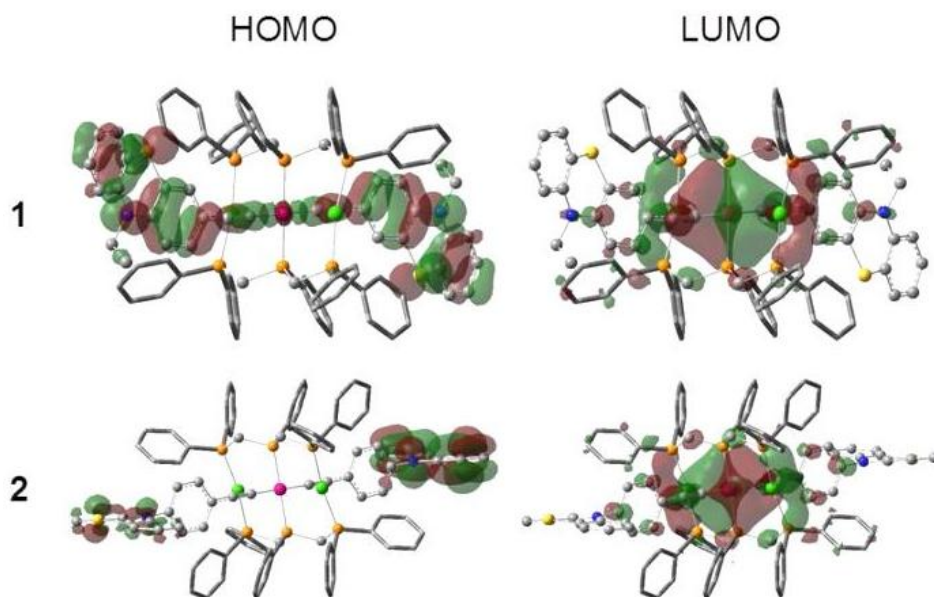


Figure S7. The HOMO and LUMO plots (isovalue = 0.025) of complexes **1** and **2** in the triplet states from TD-DFT studies

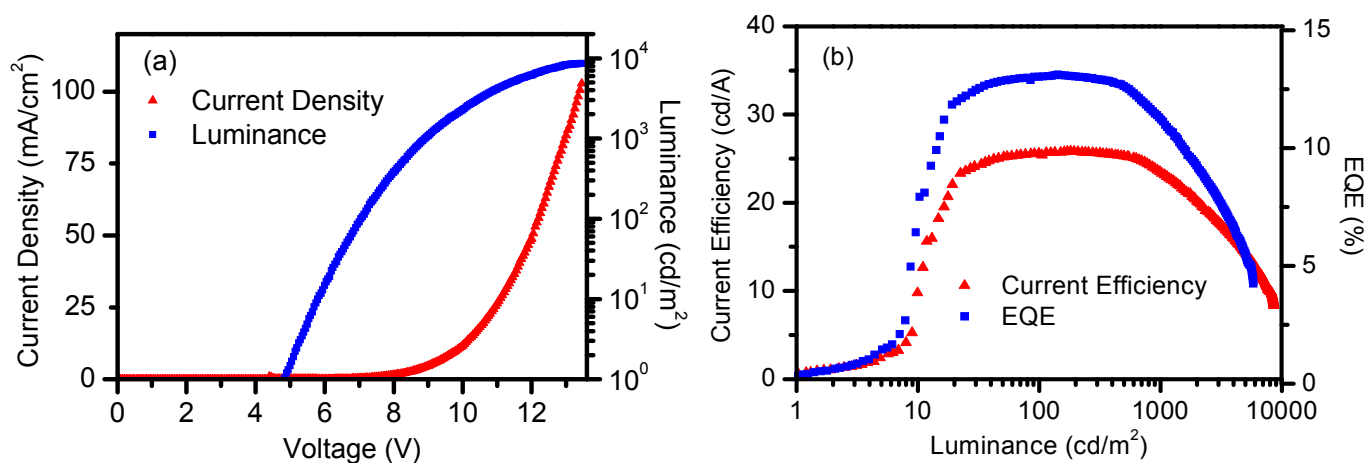


Figure S8. (a) Current density-voltage-luminance (J-V-L) characteristics. (b) Current efficiency/external quantum efficiency vs luminance for the device of complex **1** using 46% TCTA and 46% OXD-7 as a blended host.

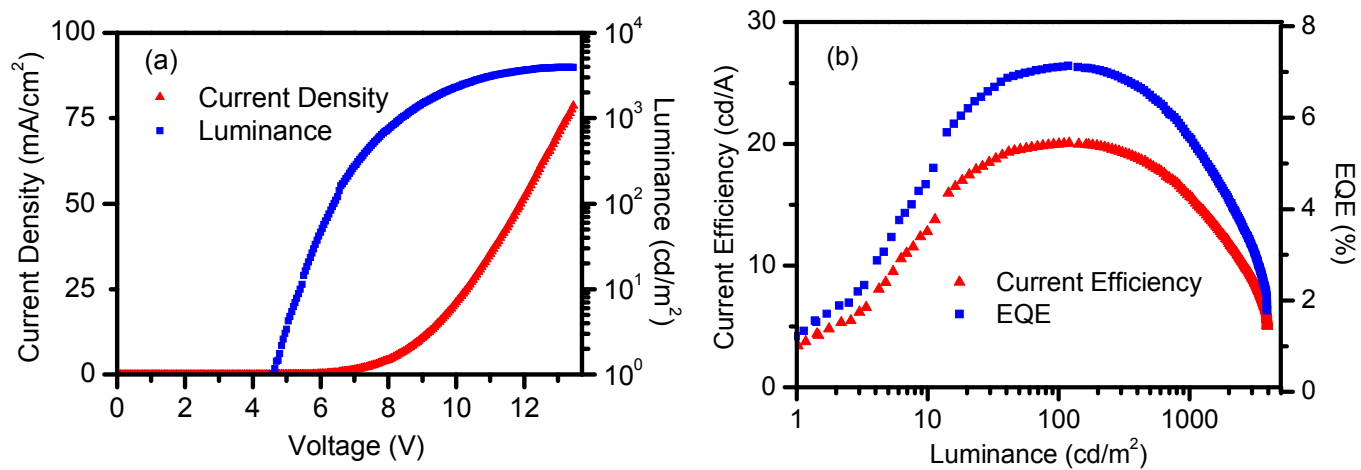


Figure S9. (a) Current density-voltage-luminance (J-V-L) characteristics. (b) Current efficiency\external quantum efficiency vs luminance for the device of complex **2** using 46% TAPC and 46% OXD-7 as a blended host.